

EVALUATION OF PHYSICO-MECHANICAL, WATER ABSORPTION AND THERMAL PROPERTIES OF *ALSTONIA MACROPHYLLA* FIBER REINFORCED POLYPROPYLENE COMPOSITES

SHETTAHALLI MANTAI AH VINU KUMAR,* JEYAKUMAR RENGARAJ** and ERUSAGOUNDER SAKTHIVELMURUGAN***

*Department of Mechanical Engineering, Sri Krishna College of Technology, Kovaipudur, Coimbatore-641042, Tamil Nadu, India

**Department of Mechanical Engineering, Sri Krishna College of Engineering and Technology, Kuniyamuthur, Coimbatore-641008, Tamil Nadu, India

***Department of Mechanical Engineering, Bannari Amman Institute of Technology, Sathyamangalam, Erode-638401, Tamil Nadu, India

✉ Corresponding author: E Sakthivelmurugan, sakthi.glen@gmail.com

Received May 4, 2024

Alkali treated *Alstonia macrophylla* fiber reinforced polypropylene (PP/AS) composite was fabricated using a hot compression moulding machine through the film stacking technique. The raw fiber was subjected to alkali treatment to enhance the strong interfacial adhesion with the PP matrix. Alkali treated fiber at five levels of fiber loading (10, 20, 30, 40 and 50 vol%) was used for composite fabrication. The fabricated composites were designated as Neat PP, PP10AS, PP20AS, PP30AS, PP40AS, and PP50AS, respectively. Mechanical test results conducted in accordance with the ASTM standards revealed that tensile strength, flexural strength, impact toughness of the PP/AS composites increased with an increase in fiber loading. However, beyond 40 vol% of fiber loading, mechanical properties deteriorate. Of the prepared laminates, PP40AS composite outperformed other laminates, with 20.14%, 274.2% and 314.42% improvement in the tensile strength, flexural strength, and impact strength, respectively, when compared to neat PP laminates. The moisture absorption rate increased with the increase in fiber loading, as it leads to an increment in the number of hydroxyl groups in PP/AS composites. TGA results showed that the thermal stability of the PP laminate improved upon impregnation with alkali treated fiber. The final thermal degradation temperature of the PP/AS composite increased from 437.7 °C to 445.2 °C. FESEM analysis revealed the major mechanism endured by the PP/AS specimens during mechanical failure.

Keywords: *Alstonia macrophylla*, alkali treatment, polypropylene, FESEM, TGA, water absorption

INTRODUCTION

In the past decades, synthetic fiber based composites (SFCs) have been utilized in many fields, such as aerospace, automobiles, marine, etc., for manufacturing parts. The use of such composites has harmful effects on the environment because of their characteristics.^{1,2} To safeguard the environment, government agencies have implemented strict rules and policies on the use of SFCs across the globe. As per governmental regulations, researchers are seeking to develop eco-friendly and biodegradable materials.³ Through their efforts, natural fiber based composites (NFCs) were developed as

environmentally friendly materials, which can serve as an alternative to SFCs in many fields. Normally, natural fibers can be derived from bark, stem, leaf stalk, seed pods, flowers, fruits, and roots of plants. The most commonly used natural fibers are sisal, banana, bamboo, jute, flax, hemp, kenaf, etc.^{4,5} Composites made from these natural fibers offer many distinct advantages over synthetic fibers, such as low density, lower cost, high specific strength, biodegradability, and renewability.

As matrix material for fiber-based composites, researchers often prefer thermoplastics over

thermosets due to lower production costs and ease of processing.^{6,7} Polypropylene (PP) is a thermoplastic material that has more benefits compared to other plastic materials, including good mechanical properties, lower cost, recyclability, flame resistance, good dimensional stability, and higher thermal stability. Composite materials fabricated with PP have superior mechanical properties, compared to other plastic materials, in terms of tensile, flexural, and impact strength. Hence, it is a good choice to use PP as a matrix material for making natural fiber polymer composites over other plastic materials.^{8,9}

Another aspect in fabricating composites is that the polymers used as matrix are hydrophobic in nature and non-polar, whereas the fibers are hydrophilic and polar. As a result, fibers are not uniformly dispersed in the polymer matrix, such as polypropylene. So, it is very important to enhance the interfacial adhesion strength between the fiber and the polymer matrix. This can be resolved by employing the appropriate chemical treatments, namely silane, alkaline, and other acid treatments.^{10,11}

Moreover, the overall properties of NFCs can be improved by modifying the physico-chemical properties of the fiber and the polymer matrix. In this context, many researchers have contributed to improving the properties of NFCs by employing different architectures of the fibers, fiber orientation, different stacking sequences, types of fibers and polymer matrix, hybridization of fibers, *etc.*¹² Wang *et al.* investigated the effect of silane treatment on the mechanical properties and thermal behavior of composites containing bamboo fiber reinforced polypropylene. The application of silane treatment resulted in an enhancement of the adhesion between the fiber and matrix in the bamboo fiber reinforced polypropylene composites, thus leading to improved mechanical properties and thermal stability. Out of the three tested silane coupling agents, it was determined that the methyl-terminated silane (KH570) was the most effective in enhancing interfacial adhesion and increasing the tensile strength and flexural strength of the composites. The incorporation of 5% KH570 silane-treated bamboo fibers resulted in a significant increase in both tensile strength (15.4%) and flexural strength (23.6%) compared to composites with untreated fibers.¹³ Margoto *et al.* performed a study to assess the impact of incorporating jute fabric layer reinforcement and

the addition of maleic anhydride on the mechanical properties of polypropylene composites. The results revealed that the inclusion of two jute fabrics and 30% MAPP led to a significant enhancement in both tensile and flexural strength compared to earlier jute PP composites. Moreover, these composites exhibited remarkable thermal stability and a reduced melting enthalpy, making them highly favorable for composite manufacturing processes.¹⁴ Wang *et al.* investigated the mechanical characteristics of polypropylene composites reinforced with woven bamboo fiber (WBF). The composites featuring alkali-treated bamboo fibers demonstrated superior tensile strength in comparison with those with untreated bamboo fibers. The longitudinal direction exhibited approximately twice the tensile strength and modulus of the transverse direction. Moisture was found to significantly impact the mechanical properties of the composites, potentially leading to degradation.¹⁵ Madhavi *et al.* conducted a study to evaluate the effect of the coupling agent MAPP on bamboo-polypropylene composites. The focus of the study was specifically on the dispersion and surface wetting of bamboo particles in the PP matrix. The findings of this investigation demonstrated that effective chemical bonding between PP, MAPP, and bamboo particles played a significant role in enhancing the mechanical strength of the composites. Moreover, the utilization of MAPP also contributed to the improvement of the interfacial chemical bonding between bamboo and polypropylene, leading to enhanced flexural strength and thermal stability of the composites.¹⁶ Chatterjee *et al.* performed a study to examine the impact of using PP sheets on the tensile strength and thermal behavior of PP-Jute laminate composites. The composites displayed enhanced tensile strength in comparison with the pure PP sheet, with the highest tensile strength achieved when utilizing 2 plies, 10% fiber loading, and 3 cm cut length of fibers. The most favorable outcomes in terms of tensile results and storage moduli were observed in the 2-ply composites across all levels of fiber loading. However, mechanical properties suffered in the case of 4-ply composites due to polymer degradation resulting from repeated processing.¹⁷

In search of new sources of natural fibers, the present study explored the use of cellulosic fiber previously derived from dry seed pods of *Alstonia macrophylla* (AS). The extraction process of the

cellulosic fiber and its characteristics were detailed in our previous studies.⁵ The main objective of the present study has been to evaluate the physico-mechanical, water absorption, and thermal properties of alkali treated AS fiber reinforced polypropylene (PP/AS) composites. Also, the effects of chemical treatments and fiber loadings on these properties, as well as on the morphology of the fractured samples, are presented.

EXPERIMENTAL

Materials

The natural fiber chosen as reinforcement in the present study was extracted from dry seed pods of *Alstonia macrophylla*, originating from Sathyamangalam Taluk, Erode District, Tamil Nadu, according to a procedure described earlier.⁵ Polypropylene (PP) sheets were used as a matrix material for the fabrication of composites; and were procured from Ghanshyam Polyplast (Coimbatore, India). Images of AS fiber and PP sheets are shown in Figure 1.

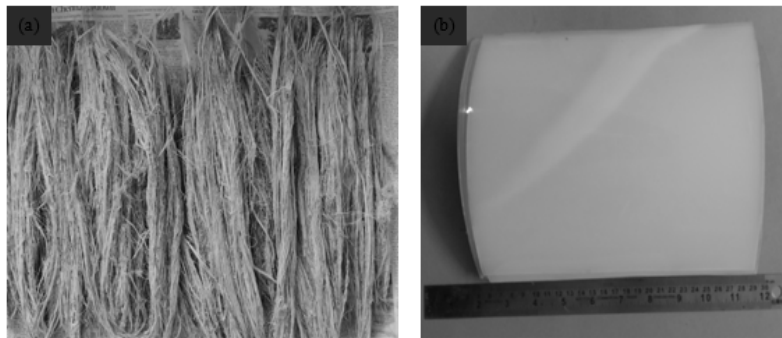


Figure 1: (a) AS fiber, (b) polypropylene sheets

Table 1
Physico-mechanical properties of AS fiber⁵

S.No.	Properties	Value	Unit
1	Cellulose	78.31	wt%
2	Hemicelluloses	11.78	wt%
3	Lignin	10.55	wt%
4	Wax	2.58	wt%
5	Ash	0.55	wt%
6	Moisture	6.88	wt%
7	Density	1.32	g/cc
8	Crystalline index	40.54	%
9	Crystallite size	2.00	nm
10	Thermal stability	269	°C
11	Tensile strength	324.89±29.41	MPa
12	Tensile modulus	2.43	GPa
13	Fiber length	28-41	mm
14	Kinetic activation energy	73.48	kJ/mol

Table 2
Physico-mechanical properties of polypropylene⁹

S.No.	Properties	Value	Unit
1	Density	0.91-0.94	g/cm ³
2	Melting temperature	160-166	°C
3	Melt flow index	3	-
4	Tensile strength	34	MPa
5	Elongation at yield	5	%
6	Flexural modulus	1310	MPa
7	Rockwell hardness, R-scale	94	-
8	Thermal conductivity	0.17	W/mK
9	Molecular weight	43.08	g/mol

The physico-mechanical properties of AS fiber and PP are detailed in Table 1 and Table 2, respectively.

Fabrication of PP/AS composites

PP/AS composites were fabricated by using the film stacking method, followed by their curing in a hot compression moulding machine. In this method, polypropylene sheets and AS fibers were placed alternately in the aluminium mould and subjected to constant pressure (25 bar) and temperature (180 °C) in a hot compression moulding machine for 15 minutes. During curing under compression, a slightly higher pressure on the scale of 0.5 bar was applied when the

melting point of PP was reached to improve the stacking ability of the laminae. Then, the whole mould was cooled to normal room temperature, and once curing was done, the PP/AS composite laminate was removed from the aluminium mould and cut into the required size for further studies. Based on fiber loading, the fabricated composites were named Neat PP, PP10AS, PP20AS, PP30AS, PP40AS, and PP50AS, respectively. The PP/AS composite fabrication process is illustrated in Figure 2. Also, the composition of PP/AS composites is detailed in Table 3.

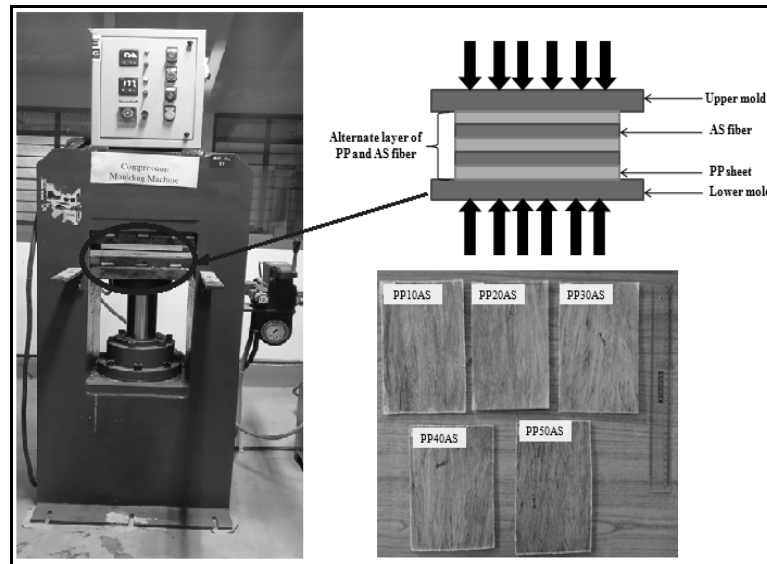


Figure 2: Fabrication process of PP/AS composite^{1,2}

Table 3
Composition of PP/AS composites^{1,2}

Sample code	Laminae		Volume fraction (vol%)		
	Type of fiber	AS fiber	PP	AS fiber	PP
Neat PP	-	-	3	-	100
PP10AS	Unidirectional fibers	2	3	10	90
PP20AS		2	3	20	80
PP30AS		4	6	30	70
PP40AS		4	6	40	60
PP50AS		6	8	50	50

Tensile test

The tensile strength of the alkali-treated PP/AS composites was determined by using a Kalpak-computerized Universal Testing Machine (UTM) (capacity: 100 kN), following the ASTM D638-14 standard.¹⁸ The test was executed at a crosshead speed of 5 mm/min. A minimum of three to five trials were conducted, and the average of their readings was calculated as the ultimate tensile strength of the PP/AS composites. Figure 3 (a) illustrates the loading setup of

the tensile samples in the Kalpak-UTM. Figure 3 (b) depicts tensile samples of the PP/AS composites prepared following ASTM standards.

Flexural test

The flexural properties of the alkali-treated PP/AS composites were studied as per ASTM D790-10 standard.¹⁸ The testing was carried out on the same Kalpak-computerized UTM, utilizing a three-point

bending configuration at a crosshead speed of 2.5 mm/min.

A minimum of three to five trials were executed, and the resultant average reading was considered the ultimate flexural strength for the PP/AS composite material. Figure 4 (a) illustrates the loading setup of the flexural samples in the Kalpak-UTM. Figure 4 (b) illustrates that flexural samples of the PP/AS composites were prepared following ASTM standards.

The flexural properties of the PP/AS composites were calculated using Equations (1) and (2), respectively:

$$\text{Flexural Strength} = \frac{3PL}{2bd^3} \text{ (MPa)} \quad (1)$$

$$\text{Flexural Modulus} = \frac{ML^3}{4bd^3} \text{ (MPa)} \quad (2)$$

where P is the load (N), L is the span length (mm), b and d are the width and thickness of the specimen (mm) respectively; M is the slope of the tangent.

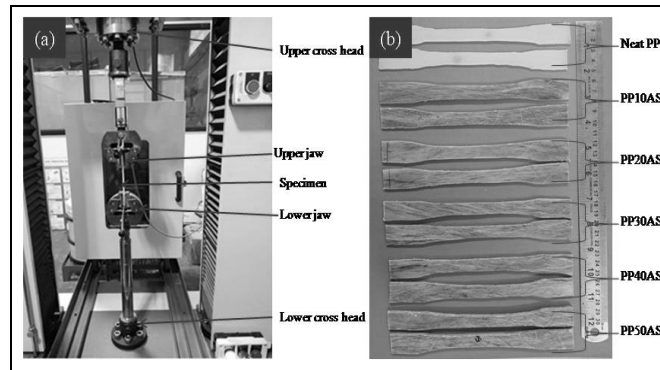


Figure 3: (a) Computer interfaced Kalpak UTM machine; (b) Tensile test samples of PP/AS composites

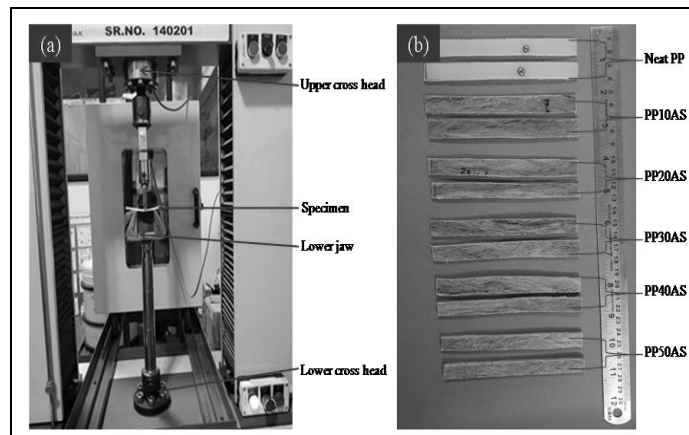


Figure 4: (a) Computer interfaced Kalpak UTM machine; (b) Flexural test samples of PP/AS composites

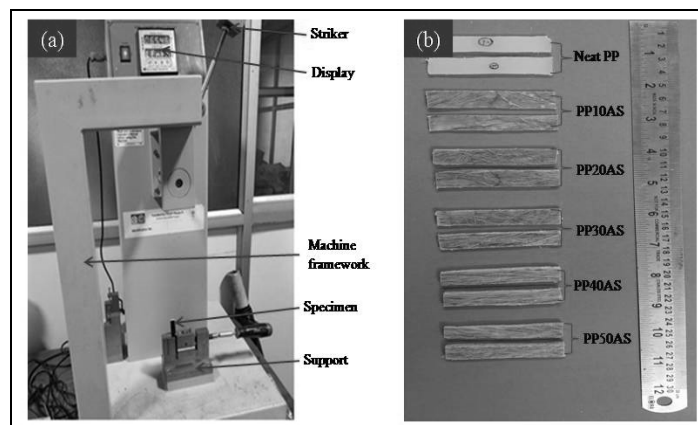


Figure 5: (a) Impact testing machine (b) Impact test samples of PP/AS composites

Impact test

The toughness assessment of the alkali-treated PP/AS composites was conducted through impact testing. A minimum of three to five trials were carried out, and the resulting average reading was designated as the composite's ultimate impact strength. In this procedure, specimens were subjected to fracture by a high-velocity pendulum released from a predetermined height. The energy absorbed by the specimen was digitally captured by the impact tester. Figure 5 (a) illustrates the Izod impact tester used for the research work. Figure 5 (b) shows that composite samples of PP/AS were prepared following the ASTM D256-10 standard.¹⁸

Shore-D hardness

A Shore-D hardness tester was utilized for determining the hardness of the alkali-treated PP/AS composites according to ASTM D2240-05.¹⁸ The test was carried out using a Durometer (Make: Hiroshima). During the testing process, the durometer indented the composite specimens at six different locations on their surfaces. The average of the six readings was considered the final hardness measurement for the composite sample.

Density

Density is a crucial fundamental characteristic of any material system, holding significance on par with mechanical properties. In engineering component design, density assumes a pivotal role as it determines material suitability based on weight considerations for various applications. The density of alkali-treated PP/AS composites was assessed following the ASTM D792-08 standard,¹⁹ employing a densometer (Milton MA124) for measurement.

Water absorption test

The water absorption test for PP/AS composites was conducted at room temperature following the ASTM standard D570.¹⁹ Distilled water and composite samples measuring 10 mm x 10 mm x 3 mm were utilized in this study. The weight of the PP/AS composite samples was measured before and after immersion in distilled water using a high-precision electronic balance (0.0001 mg). At regular intervals (every 24 hours), the samples were removed, their surfaces were cleaned using a cotton cloth, and then they were weighed on the electronic balance. This procedure was repeated until the PP/AS composite samples reached equilibrium. The calculation for the increase in the weight of the samples used the following Equation (3):

$$\text{Water absorption (\%)} = \left(\frac{\text{Final weight} - \text{Initial weight}}{\text{Initial weight}} \right) \times 100 \quad (3)$$

Thermogravimetric analysis

Thermal behavior analysis of PP/AS composites was carried out through thermogravimetric analysis (TGA) following ASTM E1131 standards,²⁰ utilizing a TGA Q50 thermal analyzer (TA Instruments, Japan). During this test, a specimen weighing between 5-8 mg was positioned on the pan and subjected to gradual heating within an enclosed furnace, ranging from room temperature to 780 °C. The heating rate was set at 10 °C/min in a nitrogen environment. The results include the thermal degradation temperatures of both Neat PP and PP/AS composites, along with their respective residuals.

RESULTS AND DISCUSSION

Tensile properties

Figure 6 (a) illustrates the variation in tensile strength and tensile modulus of Neat PP and PP/AS composites at different fiber loadings (10, 20, 30, 40, and 50 vol%). The results indicate that both tensile strength and tensile modulus of PP/AS composites increase with an increase in fiber content, compared to neat PP. However, beyond the 40% fiber loading, both properties start to reduce. This behavior is likely due to fiber agglomeration and poor interfacial bonding between the fibers and the matrix. The tensile strength of a composite material is highly sensitive to the reinforcement–matrix interactions. Good interactions between the fiber and the polymer matrix lead to good stress transfer, which can significantly increase the tensile strength. On the other hand, poor fiber–matrix interactions can lead to early fracture, as stress concentrations can build up at the interface between the fiber and the matrix.²¹ It is true that increasing fiber content beyond the optimal point (40 vol%) creates weak interfacial areas and micro spaces between the fiber and the matrix, leading to a decrease in tensile strength.

Higher fiber content also makes it difficult for the PP to fully impregnate the fibers, resulting in poor bonding and lower mechanical properties. Poor wetting further reduces stress transfer efficiency across the fiber matrix interface, causing agglomeration and blocked stress transfer.²² Consequently, there is a decreasing trend in tensile strength and tensile modulus with increasing fiber content in the PP50AS composites. Among all the PP/AS composites, PP40AS composites exhibited significantly higher tensile strength and tensile modulus, with values of 28.57±2.5 MPa and 2.47±0.50 GPa, respectively. The percentage improvements in

tensile strength and tensile modulus of PP40AS composites are 20.14% and 58.41% respectively, compared to Neat PP. Notably, the tensile modulus value exceeding 2 GPa indicates strong fiber–matrix interactions within the PP40AS composites.²¹ FESEM images of PP40AS composite tensile fractured samples have been depicted in Figure 7. The micrographs reveal that the predominant failure modes observed during the tensile testing of composite samples are fiber breakage, fiber debonding, hole formation, and matrix damage. These failure modes directly reflect the interfacial bonding strength between the fiber and matrix, which is a well-established and critical factor influencing the tensile properties of AS fiber reinforced PP composites. Moreover, the bonding characteristics at the fiber–matrix interface in composite materials are significantly affected by the surface characteristics or roughness of the fibers.²³

Flexural properties

The flexural strength and flexural modulus of Neat PP, PP10AS, PP20AS, PP30AS, PP40AS,

and PP50AS composites are presented in Figure 6 (b). The results demonstrate that the flexural properties of PP/AS composites increase with an increase in fiber content compared to Neat PP. However, both flexural strength and flexural modulus decrease beyond the optimal fiber loading (40 vol%). This trend can be attributed to the laminate structure of the PP/AS composites during the flexural test. The inner layers experience compressive forces, while the outer layers are subjected to tensile behavior, leading to the generation of tensile and compressive stresses within the composites.²⁴ During flexural loading, the AS fibers may experience compression, resulting in the occurrence of defects or kinks and leading to stress concentration sites at their ends. As the fiber loading surpasses 40 vol%, the number of crack initiation points increases due to higher stress concentration at the fiber ends. Consequently, the adhesion between the polypropylene and AS fibers weakens, resulting in a decline in flexural strength.²²

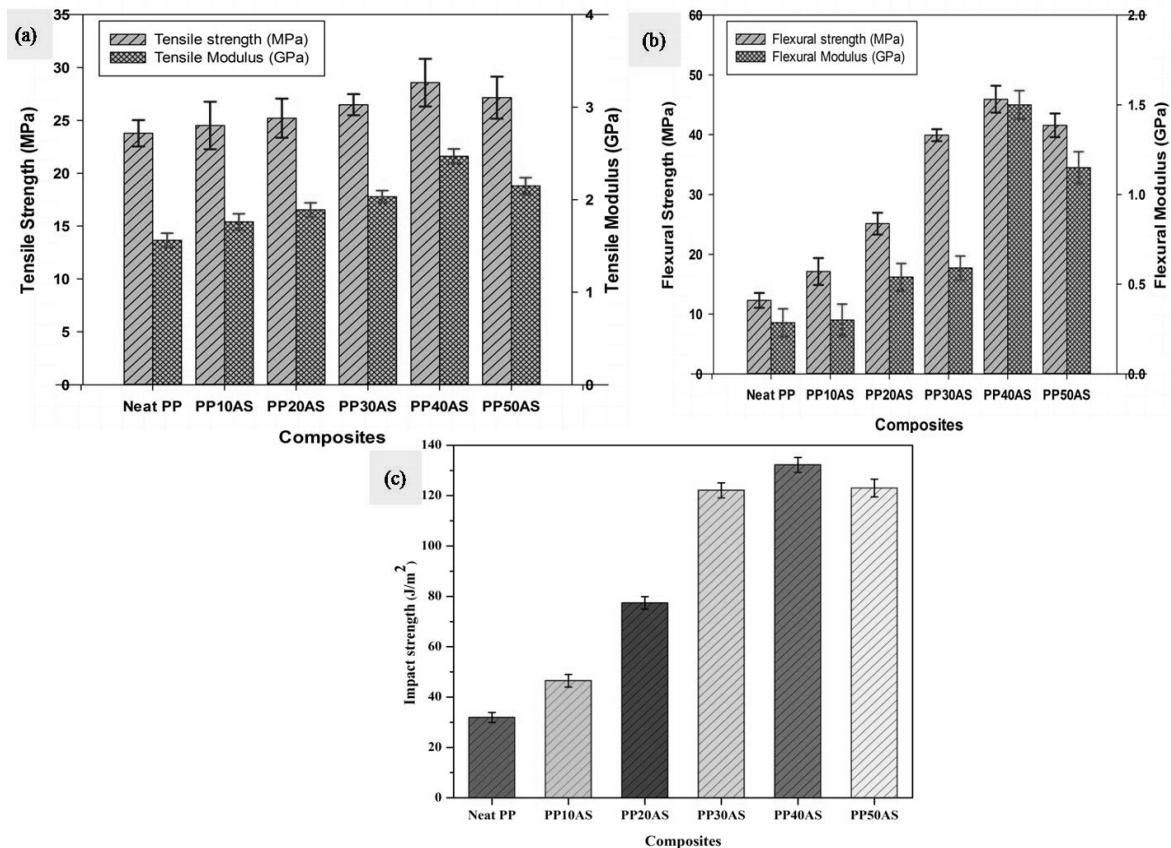


Figure 6: (a) Tensile properties, (b) Flexural properties, and (c) Impact strength of PP/AS composites at different fiber loadings

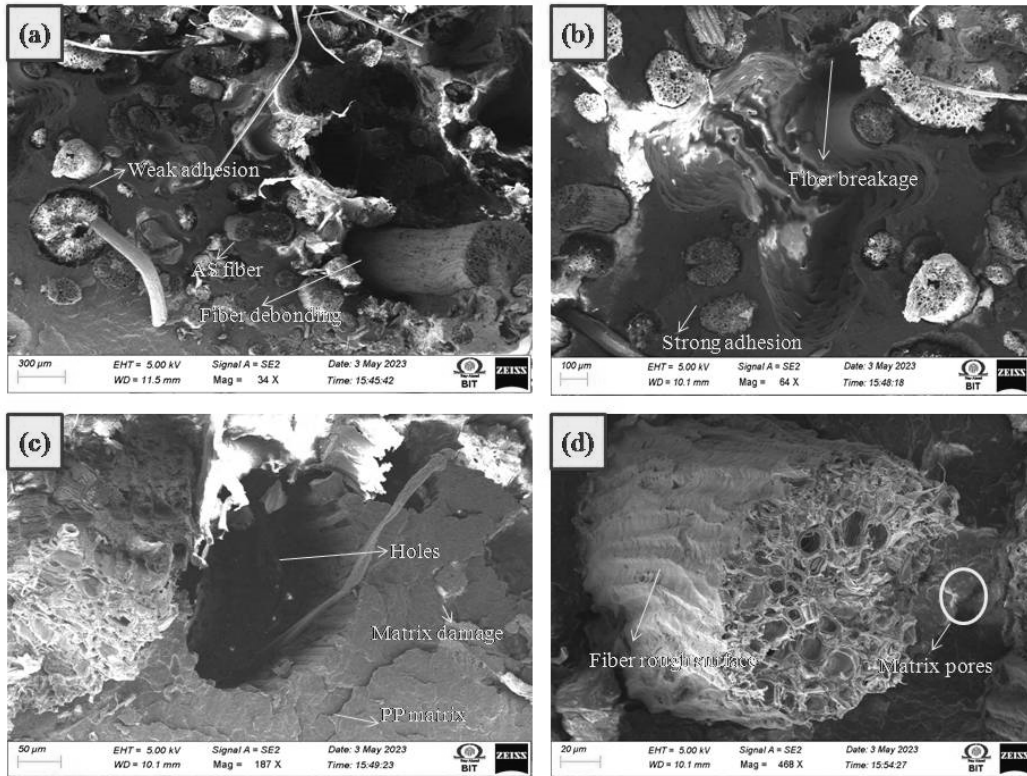


Figure 7: FESEM images of fractured tensile samples of PP40AS composites

From the plot, it is found that the PP40AS composites exhibited higher flexural strength and flexural modulus, measuring 45.93 ± 1.50 MPa and 1.49 ± 0.50 GPa, respectively. The remarkable enhancements in flexural strength and flexural modulus, compared to Neat PP are as follows: for the PP10AS, PP20AS, PP30AS, PP40AS, and PP50AS composites, the percentage improvements in flexural strength are 39.33%, 104.56%, 219.95%, 274.02%, and 238.59% respectively. Correspondingly, the percentage improvements in flexural modulus for these composites are 6.62%, 91.66%, 110.46%, 431.53%, and 308.27%. Figure 8 illustrates the FESEM images of the fractured specimens of PP40AS composites after flexural testing. The following failure phenomena have been observed in the fractured test samples: fiber breakage, pores, crack propagation, and matrix damage.

Impact strength

The impact strength of Neat PP and PP/AS composites with different fiber loadings has been depicted in Figure 6 (c). It is observed that the impact strength follows a similar trend to the

flexural strength. Impact strength refers to the material's ability to resist fracture failure under high-speed loads, making it a crucial property for composites. This property is influenced by the interaction between the AS fibers and PP during crack formation and stress transfer, with fiber loading playing a significant role.²⁵ As fiber loading increases, the impact strength of the PP/AS composites also increases, compared to that of Neat PP. The percentage improvements in impact strength for PP/AS composites, compared to Neat PP, are as follows: 45.76% for PP10AS, 142.63% for PP20AS, 282.76% for PP30AS, 314.42% for PP40AS, and 285.58% for PP50AS, respectively. PP40AS composites exhibit the highest impact strength among all the PP/AS composites, with a value of 134 ± 3 J/m². This highest impact strength at the optimal fiber loading (40 vol%) is attributed to the improved bonding between the matrix and fibers because AS fibers are uniformly dispersed in the PP matrix, serving as an efficient stress transfer medium.

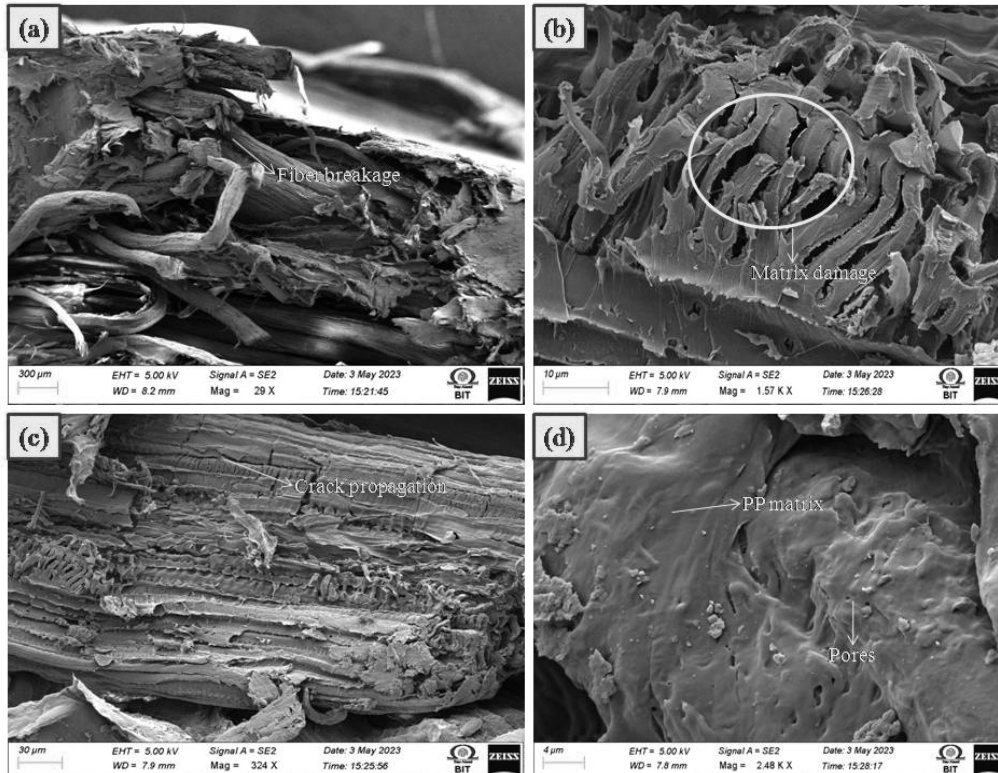


Figure 8: FESEM images of fractured flexural samples of PP40AS composites

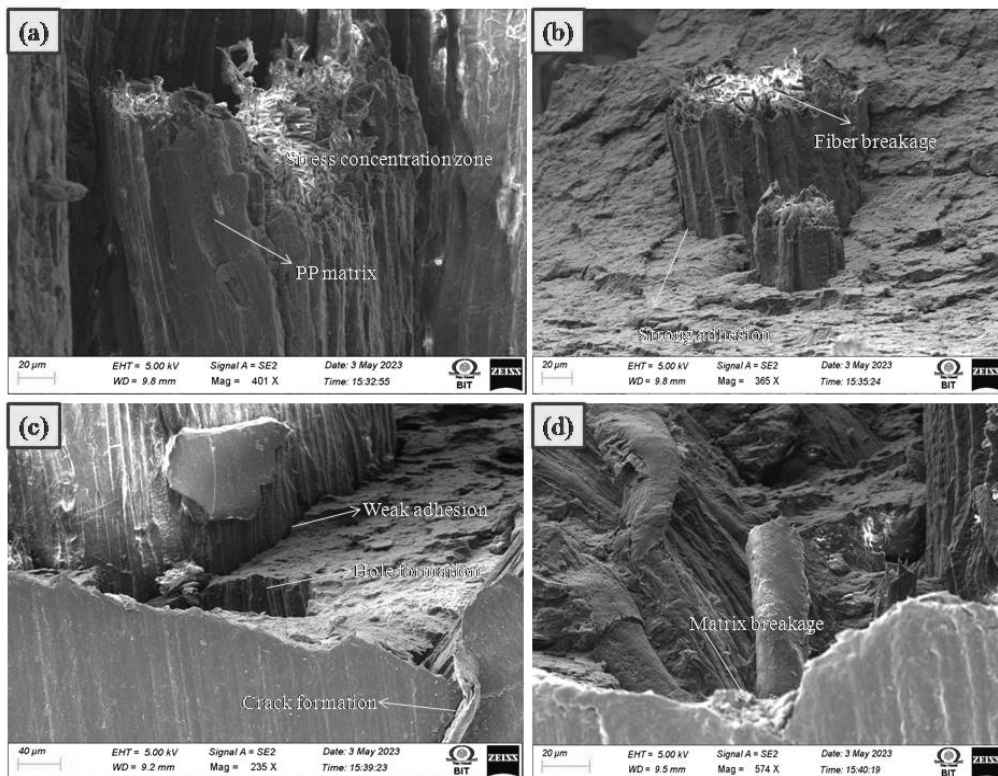


Figure 9: FESEM images of fractured impact samples of PP40AS composites

However, as the fiber loading exceeds 40 vol%, the impact strength begins to decrease. This

decreasing trend can be influenced by the emergence of voids and stress concentration

points at higher fiber concentrations. These voids and stress concentration points become initiation points for cracks during impact, leading to reduced impact resistance. The impact strength of natural fibers primarily relies on their composition, which includes factors like fiber structure, cellulose content, angle of fibrils, and cross-section. Natural fibers also contain pectin and lignin, and are abundant in hydroxyl groups, making them polar and hydrophilic materials. In contrast, polymer materials are polar, but display considerable hydrophobicity.²⁶ Fractured specimens of PP40AS composites after impact testing have been subjected to FESEM analysis to observe the failure mechanisms, as depicted in Figure 9. It is evident from the micrographs that the predominant failure modes on the fractured surfaces are matrix breakage, crack formation, hole formation, and fiber breakage.

Shore-D hardness

The shore-D hardness of Neat PP and PP/AS composites with different fiber loadings has been depicted in Figure 10. It is noted that the hardness value increases with an increase in fiber loadings. This trend may be attributed to the alkali treatment of AS fibers, enhancing their stiffness by removing impurities from their surfaces. Also, this chemical treatment ensures proper dispersion of fibers in the matrix, minimizing voids, and facilitating good interfacial bonding between the treated AS fibers and the PP matrix. Moreover, the inclusion of AS fibers in the matrix has the effect of reducing the polymer chain mobility in PP/AS composites, which ultimately contributes to an increase in hardness.⁷ In addition to that, reprocessing of the matrix material undergoes

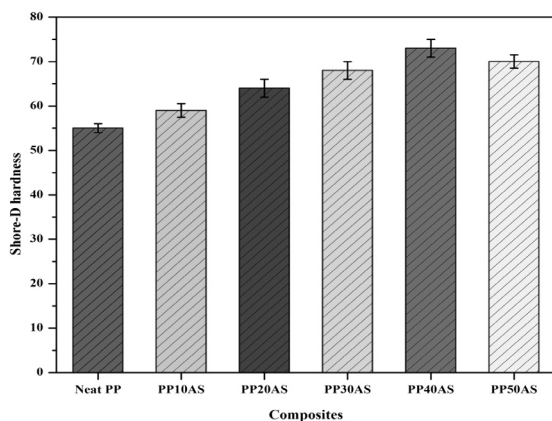


Figure 10: Shore-D hardness of PP/AS composites at different fiber loadings

multiple thermal cycles, which involve heating, mixing, and cooling, leading to a reduction in its flowability and thus improving hardness.²⁷ From Figure 10, it is noted that the PP40AS composites exhibit the highest Shore D hardness value of 73 ± 2 , in comparison with Neat PP and other PP/AS composites. The percentage improvements in hardness, compared to Neat PP, for PP10AS, PP20AS, PP30AS, PP40AS, and PP50AS composites are 7.27%, 16.36%, 23.64%, 32.73%, and 27.27%, respectively. Furthermore, at higher fiber loadings, fiber agglomeration results in poor interfacial bonding between the fiber and matrix, leading to a decrease in hardness value.²⁸ A comparison of mechanical properties of PP/AS composites over other composites is given in Table 4.

Density

The density plot for Neat PP and PP/AS composites with various fiber loadings has been depicted in Figure 11. It is observed that the density of the PP/AS composites increases with an increase in fiber loadings compared to Neat PP. This density improvement is attributed to the alkali treatment of AS fibers, which facilitates the effective interfacial bonding between the AS fibers and PP matrix. Moreover, the alkali treatment increases the cellulose content in the fibers, positively influencing the overall density of the PP/AS composites.¹⁹ Beyond the optimal fiber loading of 40 vol%, composite density decreases due to fiber agglomeration. This occurs because higher fiber content can result in air entrapment and poor fiber matrix bonding, leading to the formation of voids and a reduction in the overall composite density.

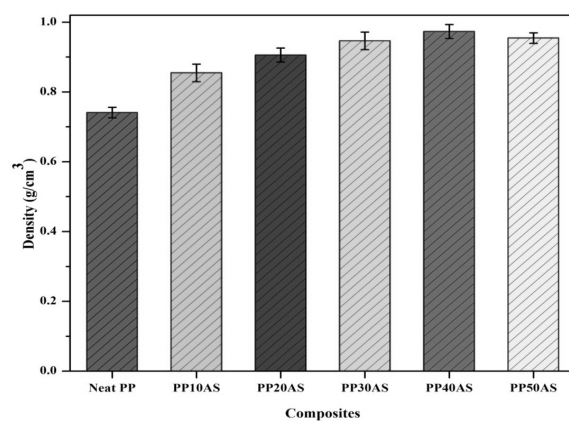


Figure 11: Density of PP/AS composites at different fiber loadings

Table 4
Comparison of mechanical properties of PP/AS composites with other composites

Composite	Mechanical properties					Hardness	Refs
	Tensile strength (MPa)	Tensile modulus (GPa)	Flexural strength (MPa)	Flexural modulus (GPa)	Impact strength (J/m ²)		
Jute/PP	23.56-29.49	0.79-2.4	42.63-48.31	1.28-3.1	22.34-39.87	-	26
Banana and pineapple/PP	25	1.17	33.5	1.23	-	75.2	28
Kenaf/PP	25.18	2.41	46.14	2.48	-	-	29
Flax/PP	30	2.2	65	2.5	63	-	30
Palm/PP	30	1.6	54	2.6	53	96	31
Bagasse/PP	15.10	-	50	0.25	-	-	32
<i>Carpinus betulus</i> /PP	33.7	1.30	60	2.3	-	-	33
<i>Alstonia macrophylla</i> /PP	28.57 ±2.5	2.47 ±0.50	45.93 ±1.50	1.49 ±0.50	134±3	73±2	Present study

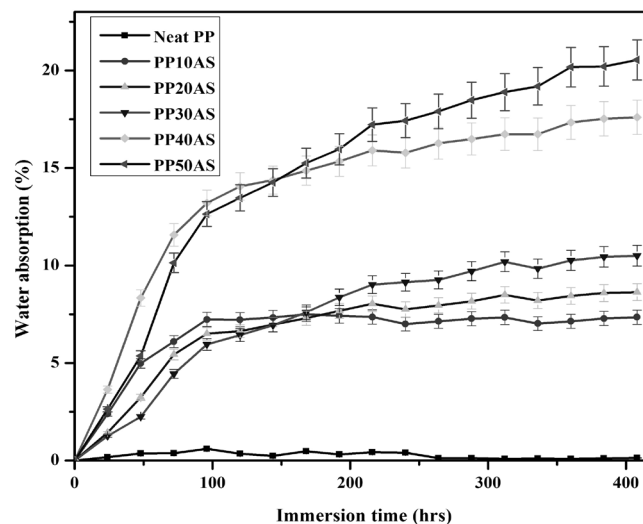


Figure 12: Water absorption of PP/AS composites at different fiber loadings

Water absorption properties of PP/AS composites

The water absorption into natural fiber composites is due to three main mechanisms: (a) water molecules move between polymer chains through microgaps; (b) water seeps into spaces and flaws between the polymer and fibers due to poor wetting and impregnation; (c) water molecules move through microcracks formed in the material during the fabrication process.¹⁹

Figure 12 illustrates that water absorption increases with an increase in the fiber loadings and immersion period for PP/AS composites. From Figure 12, it is observed that water absorption starts linearly and gradually progresses until saturation is achieved after long immersion periods. The presence of hydroxyl groups in AS fibers is accountable for the high water

absorption. As the fiber loading increases, the number of hydroxyl groups in the composite increases, leading to an increase in water absorption.^{34,35} When the fibers come into contact with moisture, they undergo a process of swelling, leading to the creation of microcracks and voids at the boundary between the fibers and the matrix.^{36,37} Consequently, this phenomenon enhances the permeability of water through the microcracks and voids. Also, the alkali treated PP/AS composites showed greater water uptake than the Neat PP. This can be attributed to the fact that the fibers' surface becomes rough due to alkaline treatment, resulting in the creation of additional pathways for water absorption.^{38,39,40} The order of water absorption of PP/AS composites is as follows: PP50AS > PP40AS > PP30AS > PP20AS > PP10AS > Neat PP.

Thermogravimetric analysis of PP/AS composites

The thermal behavior of Neat PP and PP/AS composites at different fiber loadings has been depicted in Figure 13. Neat PP undergoes a single-stage degradation process, reaching a maximum temperature of 437.6 °C, and exhibits a char yield of less than 1% following thermal analysis. This thermal degradation process of PP is solely related to the macromolecular degradation of the polymer matrix.³³ Notably, the PP/AS composites do not exhibit any mass loss before 200 °C, as the mixing temperature of the composites (190 °C) effectively evaporates moisture. The initial degradation temperature of the treated AS fiber reinforced PP composites is approximately 240 °C. The temperature corresponds to the initial weight loss (5%) of PP/AS composites as follows: Neat PP > PP10AS > PP20AS > PP30AS > PP40AS > PP50AS.

The TGA plot shows that the thermal degradation of all PP/AS composites occurs in two distinct stages. The first stage, spanning from 240 °C to 360 °C, corresponds to the thermal decomposition weight loss of AS fibers, while the second stage, from 360 °C to 480 °C, corresponds to the heat degradation of the PP matrix. The degradation stages in PP/AS composites with

higher fiber content were partially overlapped due to the uneven dispersion of the AS fibers in the PP matrix. This uneven dispersion caused the AS fibers to accumulate in some specific areas of the PP matrix. After adding AS fibers to the PP matrix, the decomposition temperature at the maximum decomposition rate of the composite increases from 440 °C to 480 °C. This improvement in thermal stability is attributed to the formation of a char during AS fibers' decomposition, which efficiently absorbs significant amounts of heat and acts as a barrier to volatile decomposition products of polypropylene.^{13,41,42} Moreover, the treated AS fiber reinforced PP composites exhibit improved thermal stability, evidenced by slightly higher maximum degradation temperature and lower char yield. This improvement is likely due to the enhanced adhesion between the fibers and the matrix resulting from the alkaline treatment.^{19,43} The temperature that corresponds to the major weight loss (75%) of PP/AS composites is as follows: PP40AS > PP50AS > PP30AS > PP20AS > PP10AS > Neat PP. Temperatures pertaining to the initial and major weight losses of the Neat PP and PP/AS composites are given in Table 5.

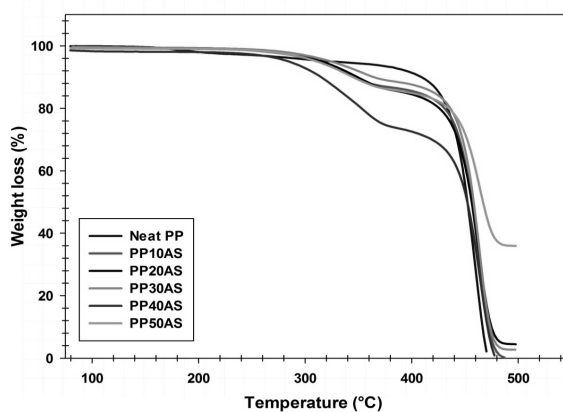


Figure 13: TGA plot for PP/AS composites at different fiber loadings

Table 5
Temperatures corresponding to initial and major weight losses of PP/AS composites

S. No.	Sample code	Initial weight loss (5%) at temperature (°C)	Major weight loss (75%) at temperature (°C)
1	Neat PP	322.6	437.7
2	PP10AS	320.6	439.7
3	PP20AS	315.1	440.1
4	PP30AS	312.2	442.1
5	PP40AS	311.7	445.2
6	PP50AS	310.1	444.6

CONCLUSION

In this study, PP/AS composites at various fiber loadings were fabricated using a hot compression moulding machine through the film stacking technique. The physico-mechanical properties of PP/AS composites increased with increasing AS fiber loadings up to 40%, then decreased. The PP40AS composites demonstrated superior physico-mechanical properties over those of Neat PP and other PP/AS composites. The percentage improvements in tensile strength, tensile modulus, flexural strength, flexural modulus, impact strength, and hardness of the PP40AS composites are 20.14%, 58.41%, 274.02%, 431.53%, 314.42%, and 32.73%, respectively, in contrast with Neat PP. Also, the failure phenomena occurring to the fractured mechanical test samples were matrix damage, fiber fracture, fiber debonding, crack propagation, and hole formation. Water absorption study results revealed that the water absorption rate increased in PP/AS composites, compared to Neat PP, due to the AS fiber loadings and inherent properties of the fiber. TGA study results indicated that the thermal stability of the PP/AS composites increased with the addition of AS fiber content. PP40AS composites exhibited good thermal stability, compared to Neat PP and other PP/AS composites. Hence, it is concluded that the PP40AS composite can be used for manufacturing automotive interior components, such as door panels, seat backs, and dashboards. The lightweight and eco-friendly nature of this composite makes it an attractive choice for reducing vehicle weight and improving fuel efficiency.

REFERENCES

- E. Sakthivelmurugan, G. Senthil Kumar, S. M. Vinu Kumar and H. Singh, *J. Braz. Soc. Mech. Sci. Eng.*, **45**, 400 (2023), <https://doi.org/10.1007/s40430-023-04339-y>
- E. Sakthivelmurugan, G. Senthil Kumar and S. M. V. Kumar, *Mater. Res.*, **26**, e20230108 (2023), <https://doi.org/10.1590/1980-5373-MR-2023-0108>
- S. M. V. Kumar and H. Singh, *Indian J. Fibre Text. Res.*, **48**, 326 (2023), <https://doi.org/10.56042/ijftr.v48i3.6057>
- V. K. Shettahalli Mantaiah, *J. Nat. Fibers*, **19**, 12415 (2022), <https://doi.org/10.1080/15440478.2022.2060404>
- E. Sakthivelmurugan, G. Senthilkumar, S. M. Vinu Kumar and H. Singh, *Cellulose Chem. Technol.*, **57**, 399 (2023), <https://doi.org/10.35812/CelluloseChemTechnol.2023.57.35>
- R. Rajiev, S. M. V. Kumar, H. Singh and E. Sakthivelmurugan, *Indian J. Fibre Text. Res.*, **48**, 396 (2023), <https://doi.org/10.56042/ijftr.v48i4.7640>
- H. U. Zaman and R. A. Khan, *Adv. J. Sci. Eng.*, **3**, 7 (2022), <https://doi.org/10.22034/22031007>
- S. Madhavi, N. V Raju and J. Johns, *Fibers Polym.*, **22**, 3183 (2021), <https://doi.org/10.1007/s12221-021-0027-9>
- H. A. Maddah, *Am. J. Polym. Sci.*, **6**, 1 (2016), <https://doi.org/10.5923/j.ajps.20160601.01>
- S. M. V. Kumar, K. L. S. Kumar, H. S. Jailani and G. Rajamurugan, *Mater. Res. Express*, **7**, 85302 (2020), <https://doi.org/10.1088/2053-1591/abaea5>
- V. K. Shettahalli Mantaiah, S. K. Kallippatti Lakshmanan and S. Kaliappagounder, *J. Nat. Fibers*, **19**, 10367 (2022), <https://doi.org/10.1080/15440478.2021.1993504>
- M. Helmi Abdul Kudus, M. M. Ratnam and H. M. Akil, *J. Reinf. Plast. Compos.*, **40**, 391 (2021), <https://doi.org/10.1177/0731684420970650>
- Q. Wang, Y. Zhang, W. Liang, J. Wang and Y. Chen, *J. Eng. Fiber. Fabr.*, **15**, 155892502095819 (2020), <https://doi.org/10.1177/1558925020958195>
- O. H. Margoto, K. D. S. Do Prado, R. C. Mergulhão, V. A. D. S. Moris and J. M. F. de Paiva, *J. Nat. Fibers*, **19**, 1792 (2022), <https://doi.org/10.1080/15440478.2020.1788489>
- B. J. Wang and W. Bin Young, *Fibers Polym.*, **23**, 155 (2022), <https://doi.org/10.1007/s12221-021-0982-1>
- S. Madhavi, N. V. Raju and J. Johns, *Fibers Polym.*, **22**, 3183 (2021).
- A. Chatterjee, S. Kumar and H. Singh, *Compos. Commun.*, **22**, 100483 (2020), <https://doi.org/10.1016/j.coco.2020.100483>
- J. D. James D. S. Manoharan, G. Saikrishnan and S. Arjun, *J. Nat. Fibers*, **17**, 1497 (2020), <https://doi.org/10.1080/15440478.2019.1581119>
- C. E. Njoku, J. A. Omotoyinbo, K. K. Alaneme and M. O. Daramola, *J. Reinf. Plast. Compos.*, **40**, 341 (2021), <https://doi.org/10.1177/0731684420960210>
- P. Vasanthkumar, N. Senthilkumar, K. Palanikumar and N. Rathinam, *J. New Mater. Electrochem. Syst.*, **22**, 25 (2019), <https://doi.org/10.14447/jnmes.v22i1.a06>
- E. Fages, S. Gironés, L. Sánchez Nacher, D. García Sanoguera and R. Balart, *Polym. Compos.*, **33**, 253 (2012), <https://doi.org/10.1002/pc.22147>
- T. Berhanu, P. Kumar and I. Singh, in *Procs. 5th Int. 26th All India Manuf. Technol. Des. Res. Conf.*, 2014, p. 2
- D. Varshney, K. Debnath and I. Singh, *Int. J. Surf. Eng. Mater. Technol.*, **4**, 2249 (2014)
- H. Awais, Y. Nawab, A. Amjad, A. Anjang, H. Md Akil et al., *Compos. Part B Eng.*, **177**, 107279 (2019), <https://doi.org/10.1016/j.compositesb.2019.107279>

- ²⁵ Y. Feng, Y. Hu, G. Zhao, J. Yin and W. Jiang, *J. Appl. Polym. Sci.*, **122**, 1564 (2011), <https://doi.org/10.1002/app.34281>
- ²⁶ M. R. Rahman, M. M. Huque, M. N. Islam and M. Hasan, *Compos. Part A Appl. Sci. Manuf.*, **39**, 1739 (2008), <https://doi.org/10.1016/j.compositesa.2008.08.002>
- ²⁷ M. K. Lila, A. Singhal, S. S. Banwait and I. Singh, *Polym. Degrad. Stabil.*, **152**, 272 (2018), <https://doi.org/10.1016/j.polymdegradstab.2018.05.001>
- ²⁸ M. Rahman, S. Das and M. Hasan, *Adv. Mater. Process. Technol.*, **4**, 527 (2018), <https://doi.org/10.1080/2374068X.2018.1468972>
- ²⁹ M. N. Akhtar, A. B. Sulong, M. K. F. Radzi, N. F. Ismail, M. R. Raza *et al.*, *Prog. Nat. Sci. Mater. Int.*, **26**, 657 (2016), <https://doi.org/10.1016/j.pnsc.2016.12.004>
- ³⁰ M. Jolly and K. Jayaraman, *Int. J. Mod. Phys. B*, **20**, 4601 (2006), <https://doi.org/10.1142/S0217979206041756>
- ³¹ M. Haque, S. Islam, N. Islam, M. Huque and M. Hasan, *J. Reinf. Plast. Compos.*, **29**, 1734 (2010), <https://doi.org/10.1177/0731684409341678>
- ³² S. Subramonian, A. Ali, M. Amran, L. D. Sivakumar, S. Salleh *et al.*, *Adv. Mech. Eng.*, **8**, 1 (2016), <https://doi.org/10.1177/1687814016664258>
- ³³ M. Atagur, Y. Seki, Y. Pasaoglu, K. Sever, Y. Seki *et al.*, *Polym. Compos.*, **41**, 1925 (2020), <https://doi.org/10.1002/pc.25508>
- ³⁴ M. M. Haque, M. Hasan, M. S. Islam and M. E. Ali, *Bioresour. Technol.*, **100**, 4903 (2009), <https://doi.org/10.1016/j.biortech.2009.04.072>
- ³⁵ J. Zhang, W. Li, L. Wang and R. Zhang, *BioResources*, **18**, 4 (2023), <https://doi.org/10.15376/biores.18.1.4-5>
- ³⁶ H. N. Dhakal, Z. Y. Zhang and M. O. W. Richardson, *Compos. Sci. Technol.*, **67**, 1674 (2007), <https://doi.org/10.1016/j.compscitech.2006.06.019>
- ³⁷ R. S. Chen, A. A. Al-Talib, M. A. I. Moustafa, M. I. M. Al-Natsheh and S. Gan, *Cellulose Chem. Technol.*, **58**, 339 (2024), <https://doi.org/10.35812/CelluloseChemTechnol.2024.58.33>
- ³⁸ C. Wang, Z. Ren, S. Li and X. Yi, *Aerospace*, **5**, 93 (2018), <https://doi.org/10.3390/aerospace5030093>
- ³⁹ T. Sullins, S. Pillay, A. Komus and H. Ning, *Compos. Part B Eng.*, **114**, 15 (2017), <https://doi.org/10.1016/j.compositesb.2017.02.001>
- ⁴⁰ S. A. Mohamed, M. El-Sakhawy and S. Kamel, *Cellulose Chem. Technol.*, **52**, 423 (2018), [https://www.cellulosechemtechnol.ro/pdf/CCT5-6\(2018\)/p.423-431.pdf](https://www.cellulosechemtechnol.ro/pdf/CCT5-6(2018)/p.423-431.pdf)
- ⁴¹ A. L. De Lemos, C. J. Mauss and R. M. C. Santana, *Cellulose Chem. Technol.*, **51**, 711 (2017), [https://www.cellulosechemtechnol.ro/pdf/CCT7-8\(2017\)/p.711-718.pdf](https://www.cellulosechemtechnol.ro/pdf/CCT7-8(2017)/p.711-718.pdf)
- ⁴² J. Zhang, C. Mei, R. Huang, X. Xu, S. Lee *et al.*, *J. Vinyl Addit. Technol.*, **24**, 3 (2018), <https://doi.org/10.1002/vnl.21516>
- ⁴³ J. Zhang, Q. Wu, G. Li, M.-C. Li, X. Sun *et al.*, *RSC Adv.*, **7**, 24895 (2017), <https://doi.org/10.1039/C7RA03327C>